Effects of High Pressure, Uniaxial Stress, and Temperature on the Electrical Resistivity of *n*-GaAs

A. R. HUTSON, A. JAYARAMAN, AND A. S. CORIELL
Bell Telephone Laboratories, Murray Hill, New Jersey
(Received 3 August 1966)

We have used a piston-cylinder apparatus to measure the resistivity of GaAs plates as a function of stress up to 50 kbar. Below 37 kbar our stress is hydrostatic, and above 37 kbar it has a uniaxial component. For sulfur-doped, floating-zone-purified GaAs the resistivity of (111) plates rises until it attains a constant value with increasing stress at 38 kbar, whereas for (100) plates it *decreases* above 38 kbar. We conclude that conduction takes place in [100] valleys at high pressure. The ratio of the "saturation" resistivity of (111) plates to resistivity at 1 atm is due to both the lower mobility in the [100] valleys and carrier "freeze-out" on sulfur donors which are deep with respect to the [100] valleys. The amount of carrier "freeze-out" was determined from the temperature dependence of the resistivity at 50 kbar. We conclude that the mobility in the [100] valleys is about 110 cm²/V-sec. We have used an empirical equation of state to correct for the pressure dependence of the compressibility and have obtained a value of 8.4 eV/(unit strain) for the rate of closure of the [000] and [100] band-edge points. Measurements on GaAs in which the Fermi level is locked to a deep donor at atmospheric pressure yielded a value of 8.15 eV/(unit strain) for the upward motion of the [000]-band minimum with pressure.

I. INTRODUCTION

IT is well known that the lowest conduction-band minimum for GaAs is at the center of the Brillouin zone (BZ) and that upon application of hydrostatic pressure, this minimum moves up in energy. At sufficiently high pressure it is believed that the lowest conduction band consists of equivalent valleys located along the ⟨100⟩ axes of the BZ. Ehrenreich[1] has analyzed the early electron-transport, optical, and pressure data relevant to this picture of the band structure of GaAs.

Our interest in the effect of pressure on the electrical properties of *n*-type GaAs arose in the course of an investigation of the mechanism of the Gunn Effect. Our preliminary experiments[2] showed that for some GaAs samples, the resistivity increased exponentially with pressure even at low pressures. These samples were clearly not suitable for the experimental observation of the decrease in Gunn-effect threshold voltage with pressure.[3] Preliminary experiments also showed that we could observe a saturation value for the resistivity at about 40 kbar for all samples, and that nonhydrostatic effects in our pressure medium could be utilized for qualitative piezoresistance analysis of the conduction-band symmetry at high pressures.

This study is chiefly devoted to two GaAs crystals which we believe exhibit two extreme examples of the way in which electrical resistivity varies with hydrostatic pressure. The first crystal to be discussed exhibited a rapid, nearly exponential increase in resistivity with pressure from atmospheric pressure up to about 38 kbar where the resistivity saturated at about 2×10^6 times its atmospheric value. This behavior is similar to that reported by Sladek[4] up to 6 kbar; however, our rate of increase of log resistivity with pressure is considerably steeper than his. The second crystal showed a slow linear increase in resistivity with pressure up to 10 kbar in quantitative agreement with Sagar's[5] elastoresistance measurements. Above 10 kbar, the resistivity increased rapidly with pressure, and then leveled off at 85 to 100 times the atmospheric pressure value at about 38 kbar. This behavior is qualitatively similar to that observed by Howard and Paul up to 30 kbar as reported by Ehrenreich[1] and by Paul.[6] However, the resistivity ratios (with respect to atmospheric pressure) measured by Howard and Paul are significantly higher than ours in the range from 20 to 30 kbar (amounting to nearly a factor of 3 at 30 kbar). One of their samples in particular appears to show an anomalously large resistivity below 10 kbar. According to Paul,[6] unpublished nonhydrostatic measurements to pressures higher than 30 kbar by Howard showed a saturation of the resistivity ratio at a value of 600.

We believe that the exponential increase in resistivity of our first sample is almost entirely due to a decrease in the number of conduction electrons with pressure, whereas the resistivity of our second sample shows chiefly the effect of increasing effective mass in the valley at $\mathbf{k}=0$ up to 10 kbar and then the effects of *both* electron transfer to valleys located along ⟨100⟩ directions in $\mathbf{k}$ space *and* a decrease in the total number of conduction electrons. The differences between our data and those of Howard and Paul we ascribe to differences in the amount of conduction-electron "freeze-out" with pressure. Ehrenreich's[1] interpretation of Howard and Paul's resistivity data did not include the carrier "freeze-out" effect and, hence, tended to underestimate the mobility of carriers in the [100] conduction-band minima.

[1] H. Ehrenreich, Phys. Rev. **120**, 1951 (1960).
[2] A. R. Hutson, A. Jayaraman, and J. H. McFee, Bull. Am. Phys. Soc. **9**, 646 (1964).
[3] A. R. Hutson, A. Jayaraman, A. G. Chynoweth, A. S. Coriell, and W. L. Feldmann, Phys. Rev. Letters **14**, 639 (1965).
[4] R. J. Sladek, Phys. Rev. **140**, A1345 (1965); and in *Proceedings of the International Conference on the Physics of Semiconductors, Paris, 1964*, edited by M. Hulin (Dunod Cie., Paris, 1964).
[5] A. Sagar, Phys. Rev. **112**, 1533 (1958).
[6] W. Paul, J. Appl. Phys. Suppl. **32**, 2082 (1961).

II. EXPERIMENTAL

Pressure was generated by a new technique which makes use of a Teflon cell to contain the fluid pressure medium in a conventional piston-cylinder apparatus. With this technique, one can reach higher hydrostatic pressures and, further, take advantage of the uniaxial component of stress which appears after the fluid medium freezes. In Fig. 1, a schematic diagram of the pressure chamber with the Teflon cell assembly in position is shown. The figure shows the materials used and relative dimensions. Consistent with lower frictional correction and effective containment of the fluid, the optimum thickness of the cell walls are 50 and 100 mils for $\frac{1}{2}$- and 1-in.-diam Teflon cells, respectively. Teflon disks on either side of the cell provide additional seals. A lead foil 1.5 mils thick is wrapped around the Teflon-pyrophyllite disk section to reduce wall friction. The pressure chamber is of tungsten carbide, press-fitted into steel binding rings and is the one normally used in the piston-cylinder device. Loading procedure and further details of the technique are discussed elsewhere.[7] To apply pressures greater than about 44 kbar, a "double-stage" technique[8] was employed in which the carbide piston was laterally supported by an annular compressed column of bismuth confined in a second pressure chamber.

For experiments at higher temperatures, a heating tape was wrapped around the pressure plate and the entire plate was heated. Temperatures up to about 200°C can be attained this way. For experiments at low temperatures, a steady stream of liquid nitrogen was directed onto the top of the pressure plate which had a copper sheet wrapped around to retain the liquid nitrogen. In this manner we can attain temperatures close to 100°K. A $\frac{1}{2}$-in.-thick transite disk inserted between the assembly and the press section provides effective thermal insulation from the press. Temperature was measured with a Chromel-Alumel couple.

Pressure Calibration

Although, in principle, pressure calibration is straightforward in a piston-cylinder device, there is always a correction to be made to the pressure computed from the gauge pressure.[9] This is due to the friction at the piston-chamber wall interface and flow properties of the pressurized assembly. In the present case, other additional sources also contribute. We have used the Bi I-II transition at 25.4 kbar for obtaining the total correction.[9] This correction is dependent upon the wall thickness, the grade of Teflon, the inside geometry of the cell, and the fluid used. For the arrangement shown

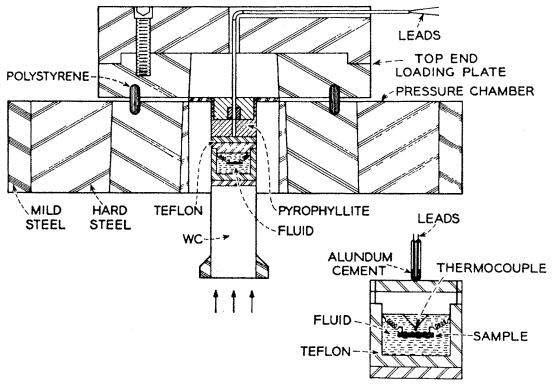

FIG. 1. Cross section of pressure chamber showing top-end loading plate and piston. The Teflon cell is shown in an expanded drawing in the right-hand corner.

in Fig. 1, which was chiefly used in the present series of experiments with *n*-pentane–isoamyl alcohol as the pressure medium, the correction was 2 kbar at 25.4 kbar, and we evaluated the true pressure for the whole range by applying a proportional correction derived from this value. The validity of this procedure was verified using a manganin gauge as the secondary standard. The response of the manganin should be linear with pressure to within about 1% up to about 30 kbar.[10] Accordingly, our plot of manganin resistance R/R_0 versus pressure, with pressure computed by applying the proportional correction mentioned above, was found to be linear.

Sample Geometry and Electrical Measurements

The semiconductor samples were square plates, about 0.150 in. on a side and with a thickness dimension of from 0.010 to 0.015 in. Crystallographic orientation of the plates was such that either a (100) or a (111) plane corresponded to the face of the plate. Ohmic electrical contacts were tin dots on GaAs (alloyed at 300°C with stannous-bromide flux), and alloyed gold dots on silicon. The dots were placed at the four corners of the upper surface of the plate. Connecting wires of enameled copper, coiled and bared at the ends, were soldered to the dots. As shown in Fig. 1, the sample plates were supported and positioned in the Teflon cell by these connecting coiled wires such that the plane of the plate was perpendicular to the axis of the piston-cylinder geometry. (The sample orientation and position is important in understanding the effects of nonhydrostatic stress in this apparatus.)

The resistivity measurements were made using two contacts on adjacent corners for current and the opposite two contacts for potential measurement. This geometry minimizes, but does not completely eliminate, effects due to changes of the current contacts. It also allows two permutations of current and voltage contacts. On changing pressure, *differences* in the change of

[7] A. Jayaraman, A. R. Hutson, J. H. McFee, A. S. Coriell, and R. G. Maines, Rev. Sci. Instr. **38**, 44 (1967).
[8] A. Jayaraman, W. Klement, Jr., R. C. Newton, and G. C. Kennedy, J. Phys. Chem. Solids **24**, 7 (1963).
[9] G. C. Kennedy and P. N. LaMori, J. Geophys. Res. **67**, 851 (1962).
[10] P. W. Bridgman, Proc. Am. Acad. Arts Sci. **74**, 1 (1940).

resistance between the two permutations of the contacts were an indication of a nonuniform stress distribution over the plate. This effect was particularly noticeable in silicone oil and silver chloride, and to some extent in the *n*-pentane–isoamyl alcohol mixture above its freezing pressure.

Both current and voltage were measured with Leeds-and-Northrup–type K-3 potentiometers and suitably sensitive null detectors.

Normally, data were taken at room temperature and at intervals of 2 or 4 kbar. When working in the low-pressure range, a transient temperature rise as large as 15° inside the cell was noted after each increment of pressure. Sufficient time was therefore allowed for the temperature to return to ambient before taking data.

Measurement of Uniaxial Stress

The stress inside the Teflon cell remains hydrostatic until the pressure medium solidifies or stiffens to a glassy state, the latter being characteristic of silicone fluids. When such conditions exist, the piston-cylinder geometry superimposes a uniaxial component of stress. For our sample geometry, this uniaxial stress is normal to the plane of the plate (and hence to the current vector). From the geometry, we can say that the uniaxial stress is symmetric about the axis of the piston. From the measurements to be discussed on silicon plates, we believe that uniaxial stress (at least for the *n*-pentane–isoamyl alcohol mixture above its freezing pressure) is essentially uniform. If the z axis corresponds to the piston axis, then the laboratory piezoresistive tensor describing the effect of the uniaxial stress in a cubic semiconductor is

$$\Pi_{xxzz}=\Pi_{yyzz}=\Pi_{12} \text{ for (100) plates}$$
$$=(\Pi_{11}+2\Pi_{12})/3-\Pi_{44}/6 \text{ for (111) plates.} \quad (1)$$

The hydrostatic effect is, of course, described by $(\Pi_{11}+2\Pi_{12})$ for all orientations.

We have used plates of phosphorous-doped, *n*-type silicon (resistivity of 4.14 Ω-cm) to ascertain the magnitude of superimposed uniaxial stress in our apparatus.

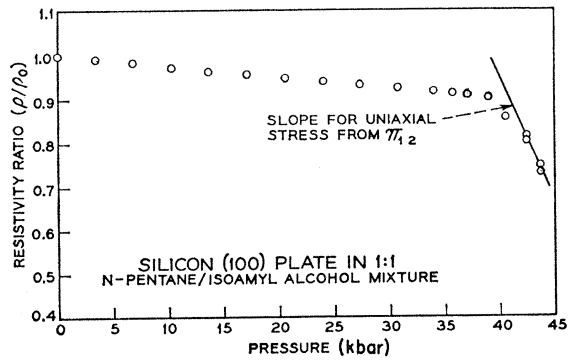

FIG. 2. Normalized resistivity versus pressure for a (100) *n*-silicon plate showing the onset of superimposed uniaxial stress above 37 kbar.

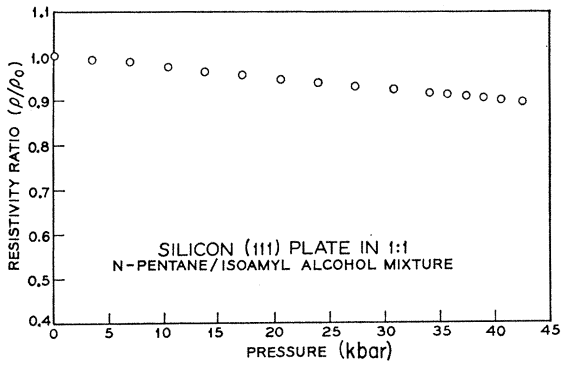

FIG. 3. Normalized resistivity versus pressure for a (111) *n*-silicon plate, to be compared with Fig. 2.

From the measurements of C. S. Smith[11] on *n*-silicon, $\Pi_{11}=-102.2\times10^{-12}$, $\Pi_{12}=+53.4\times10^{-12}$, and $\Pi_{44}=-13.6\times10^{-2}$ cm²/dyn (1 kbar$=10^9$ dyn/cm). The hydrostatic coefficient $(\Pi_{11}+2\Pi_{12})$ is small and positive (positive stress is a tension) and perhaps the best value at room temperature is 3.1×10^{-12} cm²/dyn obtained by A. C. Smith[12] isothermally.

In Fig. 2 we show the resistivity of a (100) silicon plate with a 1:1 mixture of *n*-pentane and isoamyl alcohol as the pressure medium. Up to 37 kbar, the slow decrease in resistivity is consistent with the small hydrostatic coefficient. The rapid decrease in resistivity above 37 kbar is ascribed to uniaxial stress. The slope of the resistivity-versus-pressure data becomes essentially that expected for a pure uniaxial stress. This indicates that for a medium with a relatively sharp solidification point, the incremental stress above this point is almost wholly uniaxial.

For comparison, Fig. 3 shows resistivity versus pressure in the same medium for a (111) silicon plate. There is no discernible change in slope in going from the hydrostatic to the uniaxial regime. [One might have expected a decrease in slope by a factor of 3; however, the term involving Π_{44} very nearly compensates the factor-of-3 change in the term involving $(\Pi_{11}+2\Pi_{12})$.]

Figure 4 shows resistivity versus pressure for a (100) silicon plate in silicone oil. The data clearly indicate deviation from the hydrostatic case even in the low-pressure region, and a buildup of the uniaxial stress progressively with pressure.

P-V Relationship for GaAs

In the course of our study it became clear that data on the pressure dependence of the volume for GaAs were needed. Since no such data were available, the method recently suggested by Anderson[13] was employed. Anderson has shown that the volume compression

[11] C. S. Smith, Phys. Rev. **94**, 42 (1954).
[12] A. C. Smith, thesis, Harvard University, 1958 (unpublished); also, Harvard University Division of Engineering and Applied Physics, Report H. P.-1, 1958 (unpublished).
[13] O. L. Anderson, J. Phys. Chem. Solids **27**, 547 (1966).

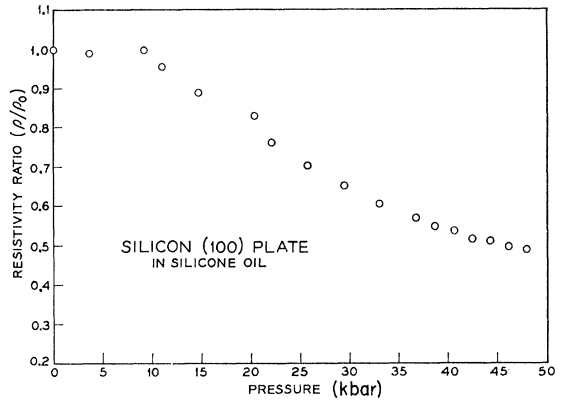

FIG. 4. Normalized resistivity versus pressure for a (100) silicon plate showing the substantial contribution of superimposed uniaxial stress with a silicone-oil working fluid.

V/V_0 can be evaluated to high pressures, making use of the pressure variation of sound velocities determined in the low-pressure range by high-precision ultrasonic techniques.[14] The parameters to be used in an appropriate equation of state are B_0, the isothermal bulk modulus, and its pressure derivative, B_0'. We used the Birch equation of state[15]

$$P=(3B_0/2)(y^7-y^5)[1-\xi(y^2-1)], \qquad (2)$$

where $y=(V_0/V)^{1/3}$, B_0 is the isothermal bulk modulus at $P=0$, and $\xi=3-\frac{3}{4}B_0'$ at $P=0$. This equation reduces to the simpler form

$$P=\frac{3B_0}{2}\left[\left(\frac{V_0}{V}\right)^{7/3}-\left(\frac{V_0}{V}\right)^{5/3}\right] \qquad (3)$$

for the special case of $B_0'=4$. For GaAs, B_0 was obtained from the data reported by Bateman, McSkimin, and Whelan.[16] The adiabatic to isothermal correction to the bulk modulus was carried out in the manner suggested by Anderson.[13] No measurements on sound-velocity variation with pressure have been reported for GaAs and, therefore, we had to assume a value for B_0'. We chose the value of 4 for B_0' which seems consistent with the measured values for analogous substances like Ge and Si.[13] Further, the choice of $B_0'=4$ has the added advantage of simplifying the Birch equation for which a computer program was readily available.[17] The computed V/V_0 is plotted against pressure in Fig. 5.

III. GaAs DATA AND ANALYSIS

Figure 6 is a useful schematic for depicting the behavior of GaAs under hydrostatic pressure. It shows, as solid parabolas for atmospheric pressure, the light-mass conduction band at $\mathbf{k}=0$ located at about 1.38 eV above the valence band and the sixfold degenerate minima located on the [100] directions in k space about 0.38 eV above the $\mathbf{k}=0$ band edge. Also shown are the positions of a very shallow, donor ground state such as sulfur, and a deep-donor Fermi level. The broken lines on the figure show the situation at about 20-kbar pressure. The $\mathbf{k}=0$ conduction band has moved substantially higher in energy. It is believed from studies of materials with analogous band structures[6,18] that the minima along [100] directions are slightly lowered in energy with increasing pressure. It is apparently also reasonable to expect (from work on deep donors in germanium and silicon)[18] that deep-state energies remain fairly constant with respect to the *valence* band under the application of pressure. Hence, a deep Fermi level controlled by deep donors and compensating acceptors is expected to remain nearly stationary with pressure. On the other hand, a shallow hydrogenic donor level would be expected to move with its associated band edge. However, a donor impurity whose ground state is nearly hydrogenic with respect to a very low-mass conduction band edge may turn out to have a deep (nonhydrogenic) ground state with respect to higher-mass band edges. In GaP whose lowest conduction-band minima are along [100] directions, and presumably is closely analogous to GaAs at very high pressures, the ionization energy of sulfur donors is reported to be 0.89[19] to 0.123 eV.[20] Our schematic Fig. 6 therefore

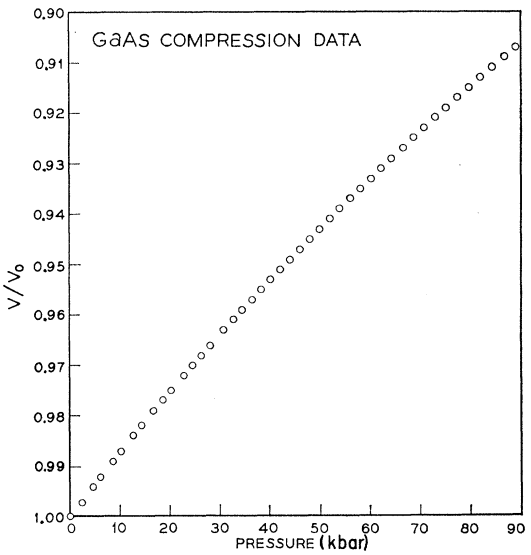

FIG. 5. Normalized crystal volume versus pressure for GaAs from the empirical Birch equation of state.

[14] H. J. McSkimin and P. Andreatch, Jr., J. Appl. Phys. **35**, 3312 (1964).
[15] F. Birch, J. Geophys. Res. **57**, 227 (1952).
[16] T. B. Bateman, H. J. McSkimin, and J. M. Whelan, J. Appl. Phys. **30**, 544 (1959).
[17] D. B. McWhan advised us on the choice of B_0', and supplied the computer program.
[18] W. Paul and D. M. Warschauer, *Solids Under Pressure* (McGraw-Hill Book Company, Inc., New York, 1963), Chap. 8.
[19] H. C. Montgomery and W. L. Feldmann, J. Appl. Phys. **36**, 3228 (1965).
[20] M. Gershenzon and R. M. Mikulyak, Solid-State Electron. **5**, 313 (1962).

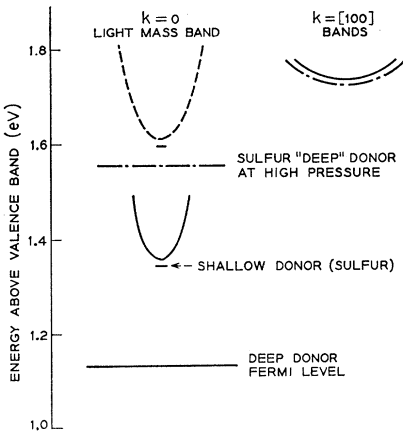

FIG. 6. Energy-level schematic for n-GaAs. The solid lines represent the band edges and levels at atmospheric pressure, while the broken lines represent them at about 20 kbar.

shows a sulfur level which is deep with respect to the [100] minima and ceases to be degenerate in energy with the continuum of the $\mathbf{k}=0$ band as that band is pushed up in energy by application of pressure. Foyt, Halsted, and Paul[21] have recently presented experimental evidence for a similar state in n-CdTe under pressure. The theory for these states when they are degenerate with a continuum has been considered by Kaplan[22] and by Peterson.[23]

High-Resistivity GaAs

The first material to be discussed was boat-grown by Monsanto and was n-type without intentional doping. Our samples had a room-temperature carrier concentration of 10^{14} cm^{-3} and a Hall mobility of about 6000 cm^2/V-sec. A measurement of the Hall effect as a function of temperature at atmospheric pressure shown in Fig. 7 shows that the carrier concentration is controlled by a deep donor. An energy of 0.217 eV is obtained from the temperature data. If we use $0.07m$ as the density-of-states effective mass, we find that at room temperature the Fermi level is 0.218 eV below the band edge. Hence, it is reasonable to assume that the Fermi level is effectively "locked" to the deep donor with the probability of considerable compensation. (We do not feel able to identify the imperfection producing this donor level; however, a level 0.2 eV below the conduction band is indicated in Fig. 7 of the paper by Blanc, Bube, and Weisberg.[24]) Models involving a Fermi level locked to a deep donor in GaAs are also discussed in Sec. 531 of Madelung's book.[25]

[21] A. G. Foyt, R. E. Halsted, and W. Paul, Phys. Rev. Letters **16**, 55 (1966).
[22] H. Kaplan, J. Phys. Chem. Solids **24**, 1593 (1963).
[23] G. A. Peterson, in *Proceedings of the International Conference on the Physics of Semiconductors, Paris, 1964*, edited by M. Hulin (Dunod Cie., Paris, 1964), p. 771.
[24] J. Blanc, R. H. Bube, and L. R. Weisberg, J. Phys. Chem. Solids **25**, 225 (1964).
[25] O. Madelung, *Physics of III-V Compounds* (John Wiley & Sons, Inc., New York, 1964).

In Fig. 8 we have plotted the logarithm of the ratio of resistivity to its atmospheric value as a function of applied pressure and as a function of crystal volume. The crystal volume was computed from the pressure measurements using the approximate Birch equation of state discussed in Sec. II. A plot of $\ln\rho/\rho_0$ is a straight line over six decades as a function of *volume*, but shows definite curvature as a linear function of pressure.

We believe that, to a first approximation, the Birch equation of state accounts for a decreasing compressibility with increasing pressure, and that the various energy levels in the crystal are more nearly linear functions of volume than of pressure. (Our use of the equation of state was originally motivated by the need to reconcile a pressure coefficient which we obtained from data between 15 and 25 kbar with existent data taken below 10 kbar. This problem in the comparison of *pressure* coefficients determined in different pressure ranges has been remarked upon on p. 247 of Ref. 18.)

If one assumes that the Fermi level remains locked at the deep-donor level, 0.217 eV below the atmospheric pressure band edge, and that this deep-donor level remains substantially unchanged with respect to the *valence band*, then the slope of $\ln\rho/\rho_0$ versus volume should yield the volume coefficient of the GaAs band gap. The slope of the straight line in Fig. 8 is -8.15 eV per unit dilatational strain. The initial slope (which is nearly linear to 10 kbar) of our equation of state is

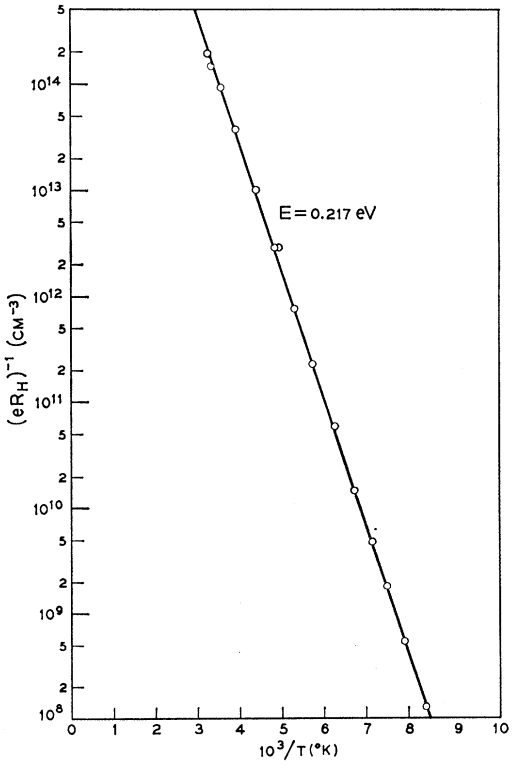

FIG. 7. Electron concentration, from Hall constant, versus $10^3/T$ for Monsanto GaAs.

$(770\ \text{kbar})^{-1}$; thus, the straight line in Fig. 8 corresponds to an initial pressure coefficient of 1.06×10^{-2} eV/kbar. This value is in remarkably good agreement with the value $(1.07\pm0.03)\times10^{-2}$ eV/kbar for the pressure coefficient of the band gap obtained from the pressure variation of the spontaneous emission from GaAs diodes by Feinleib *et al.*[26]

The high-pressure saturation value of the resistivity ratio seen in Fig. 8 is 1.8×10^6, and should be given by

$$\left(\frac{\rho}{\rho_0}\right)_{\text{sat}}=\frac{\mu_1}{\mu_2}\left(\frac{m_1^{(N)}}{m_2^{(N)}}\right)^{3/2}e^{\Delta E/kT}, \qquad (4)$$

where μ_1 and $m_1^{(N)}$ are the low-pressure values of mobility and density-of-states effective mass in the central minimum, and μ_2 and $m_2^{(N)}$ are the mobility and total density-of-states mass for the six [100] minima at high pressure. The energy ΔE is the energy separation between the [100] band edge and the Fermi level at high pressure *minus* the energy separation between the central minimum and the Fermi level at one atmosphere. Clearly $(\rho/\rho_0)_{\text{sat}}$ is a sensitive function of ΔE, and a really accurate determination of ΔE is difficult using only the data shown in Fig. 8. It appears, however, that the central and [100] band edges are equal in energy at a relative crystal volume of between 0.950 and 0.955. If we anticipate our discussion of the mobility for the [100] minima by assuming $\mu_1/\mu_2=50$ for this crystal, and use values of $m_1^{(N)}=0.07m$ and $m_2^{(N)}=1.2m$ (following Ehrenreich's[1] analysis), then $\Delta E=0.38$ eV. This value is close to the estimates of the atmospheric pressure separation of the central and [100] minima (0.38[27] and 0.36 eV[1]). Assuming a negligible pressure coefficient of the energy separation between the [100] band-edge point and the Fermi level *in this sample*, the $\Delta E=0.38$ eV and the -8.15-eV volume coefficient for the upward motion of the central minimum yield a relative crystal volume for the crossing of the band edges of 0.953 corresponding to an applied pressure of about 40 kbar. This agrees closely enough with the data shown in Fig. 8; however, it must be remembered that the working fluid freezes at 37 kbar so that the apparent band-crossing point occurs just beyond the limit of hydrostatic conditions and the validity of our equation of state.

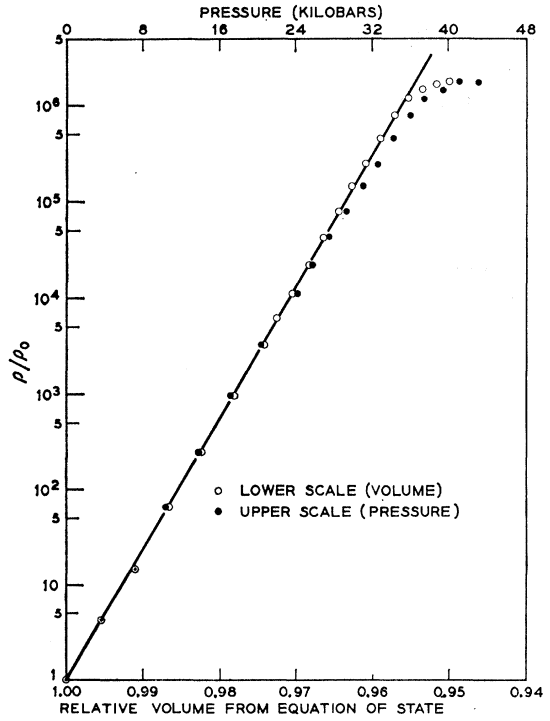

FIG. 8. Normalized resistivity versus pressure and versus volume for Monsanto GaAs controlled by a deep donor.

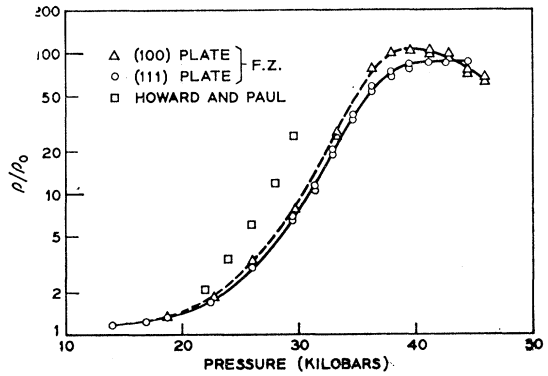

FIG. 9. Normalized resistivity versus pressure for a (100) and a (111) plate of sulfur-doped, floating-zone-purified GaAs. Data of Howard and Paul (Refs. 1 and 6) is also shown for comparison.

Sulfur-Doped GaAs

Let us now turn to the data and analysis of our other GaAs material. The samples which we shall discuss were plates oriented normal to [100] and [111] axes. They were cut from adjacent regions near the center of a GaAs ingot, grown in a graphite boat from extremely pure starting materials, including sulfur as a donor dopant. These ingots were refined by the floating-zone technique which effectively removes silicon impurity from the central portion of the ingot. This careful preparation and purification produced crystals which we believe contain only sulfur donors, partially compensated by some (unknown) acceptor levels.[28]

The samples had an atmospheric-pressure-carrier concentration of about 2.5×10^{16} cm^{-3} and a mobility at room temperature of about 4700 cm^2/V-sec. Slight differences in carrier concentration were observed between the pieces from which the (100) and (111) plates

[26] J. Feinleib, S. Groves, W. Paul, and R. Zallen, Phys. Rev. 131, 2070 (1963).

[27] L. W. Aukerman and R. K. Willardson, J. Appl. Phys. 31, 939 (1960).

[28] We are greatly indebted to J. M. Whelan and R. G. Sobers for the crystal growth and purification research which produced these samples.

were cut. Hall measurements taken from room temperature down to 20°K showed no indication of carrier freezout, in agreement with a "hydrogenic" donor binding energy of about 0.007 eV for sulfur on an arsenic site.

The resistivity ratio for the float-zoned sulfur-doped material rises sharply with pressure between about 18 and 38 kbar. This is shown in Fig. 9 for both a (100) and a (111) plate. In the low-pressure region, up to roughly 14 kbar, both orientations exhibit a small, nearly linear increase of ρ/ρ_0 with pressure. Above about 38 kbar, ρ/ρ_0 for the (111) plate remains nearly constant at a saturation value of 85. The (100) plate, however, reaches a maximum ρ/ρ_0 of about 105, and then with increasing applied stress, *decreases*. Since our working fluid freezes at about 37 kbar, the applied stress above 37 kbar is very nearly uniaxial in a direction perpendicular to the plane of our sample plate. The nearly constant value of ρ/ρ_0 above 38 kbar for the (111) plate suggests that above this pressure the light-mass, $\mathbf{k}=0$, conduction band is no longer contributing to the conductivity, and that the higher-mass band minima in which conduction is taking place remain degenerate in energy under the application of uniaxial stress along the [111] direction. The decrease in ρ/ρ_0 for the (100) plate suggests that uniaxial stress along the [100] direction removes the degeneracy of the upper band minima in such a way as to lower the resistivity measured in the plane perpendicular to the direction of compressive stress. This behavior is consistent with a model in which the conduction band of GaAs at high pressure is similar to that of silicon, in which we have noted the same sort of behavior in Sec. II for (100) and (111) plates upon freezing of the working fluid. At high pressure, the conduction band consists of six prolate ellipsoids oriented along [100] directions in $\mathbf{k}$ space, and under the additional application of a [100] uniaxial compression, the two valleys lying along the axis of compression are lowered in energy with respect to the four perpendicular valleys. The resulting imbalance in electron population among the valleys results in a lower inertial mass in directions perpendicular to the stress axis (averaged over the entire electron population) and, hence, a decrease in the resistivity measured in the plane of the plate. This behavior at high pressures *cannot* be reconciled with a model having conduction-band ellipsoids oriented along [111] directions.

During the course of our investigation, Shyam, Allen, and Pearson[29] have reported that uniaxial stress lowers the Gunn-effect threshold, with the largest effect occurring for [100] stress, the next largest for [110] stress, and the smallest effect for a [111] stress. On the basis of the "two-valley" model of the Gunn effect, this is strong evidence that the upper valleys have a [100] orientation. However, there appears to be an unexplained numerical discrepancy between their uniaxial results and our[3] hydrostatic Gunn-threshold measurements.

The simplest model for the large increase and subsequent saturation of ρ/ρ_0 would be one in which a constant concentration of conduction electrons is divided according to Maxwell-Boltzmann statistics between the [000] band and the [100] bands. A greater fraction of the carriers are "transferred" to the [100] bands as the energy difference between the two band-edge points decreases under pressure, until finally effectively all of the carriers are in the [100] band. If this model were correct, the *mobility* in the [100] band could be simply obtained from ρ/ρ_0 at saturation and the mobility at atmospheric pressure. Unfortunately, the carrier concentration does *not* remain constant with pressure between 20 and 38 kbar even for the floating-zone, sulfur-doped GaAs. One indication of carrier "freeze-out" with increasing pressure is the small, but reproducible difference between our (111) plates and our (100) plates. This difference, which is most pronounced at 38 kbar, can be seen to commence just above 20 kbar. We attribute it to a relatively small difference in donor concentration between samples obtained from slightly different parts of the original ingot. Figure 9 also shows some of the data taken by Howard and Paul[1,6] which agree very closely with ours below 20 kbar, but reach a value of ρ/ρ_0 at 30 kbar which is larger than our values by nearly a factor of 3. We believe that in the samples measured by Howard and Paul, carrier freeze-out became the dominant mechanism involved in the increase of resistivity above 20 kbar. This would also explain why Howard[6] (on a different sample) observed a saturation value of ρ/ρ_0 of 600 at very high pressures.

Determination of [100] Mobility: Effect of Carrier "Freeze-Out"

Since we were interested in obtaining a measure of the mobility of carriers in the upper [100] valleys it was important to try to obtain independent data on carrier freeze-out. We therefore measured the resistivity of a (111) plate of the float-zoned material as a function of temperature at a constant applied stress of about 50 kbar. This very high pressure, obtained by the double-stage technique, was chosen in order to eliminate the possibility of any residual conductivity arising from the [000] valley. In order to change temperature, the entire pressure-confining part of the press was heated or cooled from the outside, and the upper temperature turned out to be limited by rupture of the Teflon capsule.

The temperature dependence of the resistivity, normalized to its value at 300°K, is shown in the customary semilogarithmic plot as a function of reciprocal temperature in Fig. 10. At the lower temperatures, $\ln\rho$ versus T^{-1} is well represented by a straight line characterized by an activation energy of about 0.214 eV. For this very steep portion of the data, the temperature

[29] M. Shyam, J. W. Allen, and G. L. Pearson, IEEE Trans. Electron Devices **ED-13**, 63 (1966).

dependence of the mobility can have only a negligible effect; hence, the carrier freeze-out at high pressure occurs to a *deep* state.

We believe that this deep state is the "nonhydrogenic" ground state of the sulfur donor with respect to the [100] band edge discussed in connection with Fig. 6. Since this *is* a deep state, the chemical shift should effectively remove any valley-orbit degeneracy, leaving a singlet ground state with a spin degeneracy of 2.

Attempts to fit the data of Fig. 10 with a donor ionization energy of 0.214 eV and a spin degeneracy of 2 were not consistent with Ehrenreich's[1] estimate of 1.2 for the density-of-states mass of the six equivalent [100] valleys. It is possible that we have more than one deep-donor level at high pressure resulting from impurities which give rise only to hydrogenic, shallow levels at atmospheric pressure. However, we believe that this is unlikely in view of the floating-zone purification. A more likely explanation of this difficulty is that the ionization energy of the deep sulfur donor is temperature-dependent, so that $E_d=E_0-\alpha T$.

The fit to the data in Fig. 10 was obtained from the carrier-concentration expression

$$\frac{n(n+N_A)}{(N_D-N_A-n)}=N_c^*\,e^{-E_0/kT}, \tag{5}$$

where

$$N_c^*=[(m^{(N)}/m)^{3/2}D^{-1}\,e^{\alpha/k}]2(2\pi mkT/h^2)^{3/2}$$

contains the corrections for density-of-states mass, donor degeneracy, and the temperature coefficient. We assumed that $(N_D-N_A)=2.5\times10^{16}$ was known from the Hall measurements on this sample at atmospheric pressure, and $E_0=0.214$ eV was assumed to be equal to the activation energy of the high-pressure resistivity data *at the lowest temperature* (assuming a negligible mobility correction). Thus, Eq. (5) could be calculated for various choices of N_A and N_C^*. These calculations were facilitated by calculating the left-hand side of Eq. (5) for specific values of n and then finding the corresponding temperatures from a semilogarithmic plot of $N_Ce^{-E_0/kT}$ versus T^{-1} and the chosen value of the parameter N_C^*/N_C. In order to compare these calculations of $n(T)$ with the experimentally determined resistivities, a simple $T^{-3/2}$ dependence was assumed for the mobility. (This dependence seemed to be a fair approximation to the Hall mobilities measured by Montgomery and Feldmann[19] in GaP over our rather restricted temperature range from 180 to 380°K.) Semilogarithmic plots of $n^{-1}T^{3/2}$ were compared directly with the data of Fig. 10. Our best fit is shown in the figure. The parameters characterizing this fit were $N_A=1\times10^{16}$ and $N_C^*/N_C=3$.

The most important information obtained from this analysis was $n/(N_D-N_A)$, the ratio of carrier concentration at high pressure to its atmospheric pressure value. Our best fit yielded 0.5 for this ratio; furthermore,

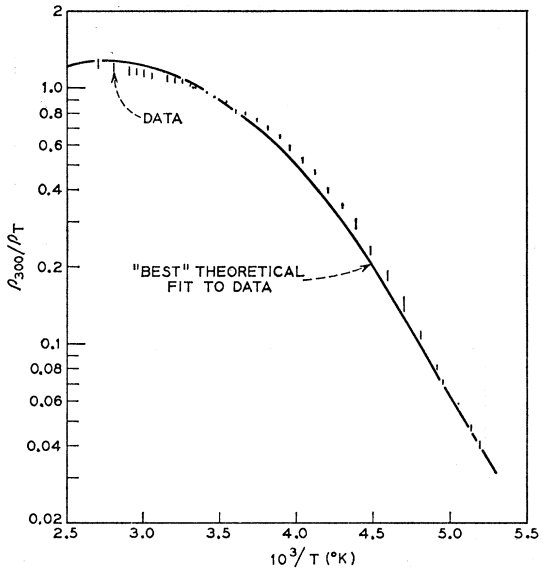

FIG. 10. Normalized resistivity versus reciprocal temperature for a (111) plate of sulfur-doped, float-zoned GaAs at 50 kbar applied pressure. The vertical bars representing the data show the spread between the two permutations of the contacts. The theoretical fit is discussed in the text.

this ratio turned out to be relatively insensitive to changes in the fitting parameters. Combining this carrier-concentration ratio with the saturation value of the resistivity ratio and the atmospheric-pressure Hall mobility, we conclude that the mobility in the [100] conduction band for our sample at high pressure is about 110 cm²/V-sec. We would expect only a small difference between this high pressure value for the [100] mobility and its value at 1 atm, which is relevant to the "two-valley" model of the Gunn effect. Except for scattering from the [100] valleys to the [000] valley, the [100] mobility would be expected to be slightly reduced by pressure, as is the case for silicon. Scattering from the [100] valleys to the [000] valley might result in a slight increase of the [100] mobility with pressure; however, this effect is of small importance for the [100] mobility, since the density of states in the [000] valley is small at all pressures. (Relaxation times for scattering of electrons in [100] valleys have been estimated by Conwell and Vassell.[30])

Our value of 110 cm²/V-sec for the mobility in the [100] conduction band disagrees with a recently quoted value of 230 cm²/V-sec obtained at high pressure by King *et al.*[31] It is possible that our value might be low because of an underestimation of the amount of carrier freeze-out, or as the result of a "mobility killer."[32]

[30] E. M. Conwell and M. O. Vassell, IEEE Trans. Electron Devices **ED-13**, 22 (1966).

[31] G. King, J. Lees, and M. P. Wasse (private communication), quoted by C. Hilsum, Phys. Letters **20**, 136 (1966).

[32] L. R. Weisberg and J. Blanc, in *Proceedings of the International Conference on Semiconductor Physics, Prague, 1960* (Publishing House of the Czechoslovakian Academy of Sciences, Prague, 1961), p. 940.

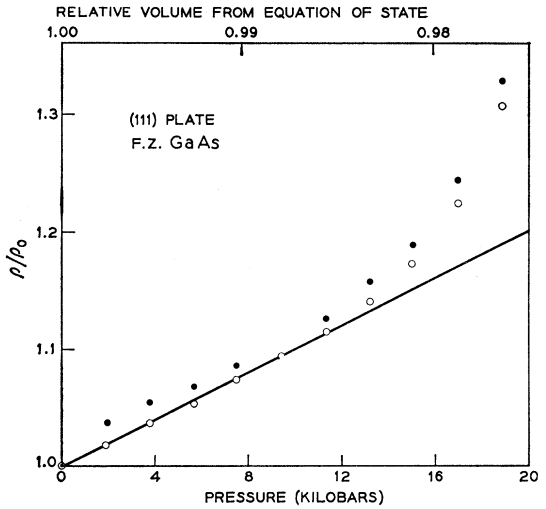

FIG. 11. Normalized resistivity versus pressure and volume plotted on an expanded scale for the low-pressure region. The solid and open circles are the data points taken with the two contact permutations. The solid line is taken to be the expected change of the resistivity due only to the effect of pressure on the mobility in the central minimum.

We may estimate the maximum effect of the "mobility killer" by comparing our atmospheric-pressure mobility of 4700 cm²/V-sec with 6000 cm²/V-sec, the value predicted by Ehrenreich[1] for the mobility in a sample with 5×10^{16} ionized impurities. We expect, however, that the mobility-killer centers (and ionized centers as well) would make a much smaller relative contribution to the scattering of [100] electrons than to the scattering of electrons in the central minimum.

It seems probable (to us) that the [100] mobility obtained by King *et al.* is too high as a result of nonhydrostatic stress above 40 kbar, where resistivity saturation takes place. [We have observed a maximum resistivity of only 35 times the atmospheric-pressure resistivity for (100) plates using silicone oil as the working fluid, and comparable nonhydrostatic effects using silver chloride.]

From our temperature data we are also in a position to evaluate the temperature coefficient of the sulfur deep-donor level. If we assume $m^{(N)}/m=1.2$ and $D=2$, then our $N_C^*/N_C=3$ yields a temperature coefficient $\alpha=1.4\times10^{-4}$ eV/deg. The sulfur donor, at high pressure, is then characterized by an ionization energy of $E_d=0.214-1.4\times10^{-4}T$ eV (T in °K), which at 300°K is equal to 0.172 eV. Both the sign of α and its magnitude, which is roughly one-third of the temperature coefficient of the energy gap for GaP,[33] seem reasonable.

From the room-temperature deep-donor ionization energy, we can estimate a minimum pressure (or strain) at which carrier freeze-out can commence. Certainly, there will be negligible freeze-out on this level when it is degenerate in energy with the continuum of the [000] band (and hence ill-defined in energy). From the density-of-states of the [000] band, the carrier concentration, and the donor concentration, we estimate that freeze-out does not commence until the [000] band edge is about $3kT$ *above* the deep-donor level. From the approximate atmospheric-pressure separation between the [100] and [000] band edges of 0.38 eV, we can roughly estimate that a strain sufficient to raise the [000] band edge by 0.29 eV is required. Using the strain coefficient of the band edge of −8.15 eV determined on the Monsanto material, we arrive at a relative volume of 0.967 or a pressure of 27 kbar for the onset of appreciable freeze-out. This estimate may be a little too big, since it neglects the expected small downward motion of the [100] band edge with pressure, and it is, of course, only approximate since we do not know the pressure coefficient of the deep-donor ionization energy, which must involve the perturbative effect of the energetically close [000] valley. However, the data shown in Fig. 9 indicate that this estimate is not too far off the mark.

The last part of the analysis will be devoted to a closer examination of the pressure dependence of ρ/ρ_0 for the floating-zone material. Figure 11 shows ρ/ρ_0 versus pressure (and volume) in the low-pressure region on a greatly expanded scale. The open and solid circles are data points for the two possible permutations of the current and voltage contacts. There is noticeable scatter for the data represented by the solid circles, which we believe is due to slight changes in effective contact area for one of the current contacts in that permutation. Fluctuations of this order of magnitude were frequently seen on different samples. The open circles are characteristic of very "quiet" contacts. We shall be concerned with the "quiet" contact data.

Below 10 kbar, ρ/ρ_0 is linear with pressure and is in agreement with Sagar's[5] measurements. This behavior is a measure of the change in mobility for carriers in the [000] valley chiefly owing to the pressure-dependent increase in effective mass. Above 10 kbar, we attribute the more rapid increase in ρ/ρ_0 to electron transfer from the [000] valley to the [100] valleys.

In order to analyze the pressure dependence of ρ/ρ_0, we must take account of the change in mobility and density of states of the [000] valley, as well as the change in the energy difference ϵ measured in units of kT, between the [000] and [100] band-edge points. We shall assume that the mobility and density of states of the [100] band do not change with pressure. Quantities pertaining to the [000] band will be labeled with the subscript 1 and those for the [100] band with the subscript 2. The conductivity of the sample is then

$$\sigma=(n_1\mu_1+n_2\mu_2)e, \tag{6}$$

where $n_1+n_2=n$ is the total free-carrier concentration. Since the Fermi level is always well below both band

[33] P. J. Dean and D. G. Thomas, Phys. Rev. **150**, 249 (1966).

edges,

$$n_1/n_2=(N_1/N_2)e^{\epsilon}, \tag{7}$$

where N_1, N_2 are the band densities of states.

The resistivity is then

$$\rho=\frac{1}{\mu_2 n}\frac{[1+(N_1/N_2)e^{\epsilon}]}{[1+(\mu_1 N_1/\mu_2 N_2)e^{\epsilon}]}, \tag{8}$$

and for $\epsilon\gg 1$, $\rho=(\mu_1 n)^{-1}$, and $\rho_0=(\mu_{10}n_0)^{-1}$. The resistivity ratio can be written in the form

$$\frac{\rho}{\rho_0}=\frac{(\mu_{10}N_1/\mu_1 N_1)e^{-\epsilon}+(\mu_{10}/\mu_1)}{(n/n_0)[1+(\mu_2 N_2/\mu_1 N_1)e^{-\epsilon}]}. \tag{9}$$

The initial behavior of ρ/ρ_0 in Fig. 11 corresponds simply to $\rho/\rho_0=\mu_{10}/\mu_1$. Then at about 10 kbar the term involving $e^{-\epsilon}$ in the numerator of the right-hand side starts to contribute. The term in the denominator involving $e^{-\epsilon}$ does not affect ρ/ρ_0 until one gets to higher pressures (smaller ϵ) since $\mu_2/\mu_1\cong 0.02$. And, from our previous estimate, n/n_0 is not expected to drop until the pressure is close to 27 kbar for our float-zoned material.

We have therefore carefully plotted $\ln(\rho/\rho_0-\mu_{10}/\mu_1)$ versus volume in Fig. 12. Extrapolation of μ_1 to pressures above 10 kbar took into account a $(-\frac{3}{2})$ power dependence of μ_1 on the effective mass (polar mode scattering) and the assumption that the mass change is linear with volume. Furthermore, since $N_1\sim m_1^{*3/2}$, the product $\mu_1 N_1$ is a constant. (It is probably sufficiently constant for our purposes even for some mixture of scattering processes.)

In Fig. 12 we see that $\ln(\rho/\rho_0-\mu_{10}/\mu_1)$ is a straight line over two decades for the data between 12 and 25 kbar. Its slope yields a value of +8.4 eV/unit dilatation for the rate of change of *energy separation* between the [000] and [100] band edges under hydrostatic pressure. On the Monsanto material the upward motion of the [000] band edge with respect to a deep state in the forbidden energy gap was characterized by a value of −8.15 eV/unit dilatation. We believe that the sum of these two values is a measure of the expected *downward* motion with pressure of the [100] band edge.

The rate of closure of the [000] and [100] band edges extrapolated to low pressures is -1.15×10^{-2} eV/kbar. We had originally made plots similar to Fig. 12 as a linear function of *pressure* and had determined a slope of 0.96×10^{-2} eV/kbar for the straight-line portion between 12 and 25 kbar. The fact that this slope was *less* than the measured rate of increase of the energy gap[26] at low pressures suggested the need to correct for the change of compressibility through an equation of state.

The intercept at a volume of unity of the lower, straight-line portion of the plot in Fig. 12 is 5×10^{-5} and should be equal to $(N_2/N_{10})e^{-\epsilon_0}$. Assuming density-of-states masses of $1.2m$ and $0.07m$, this yields an

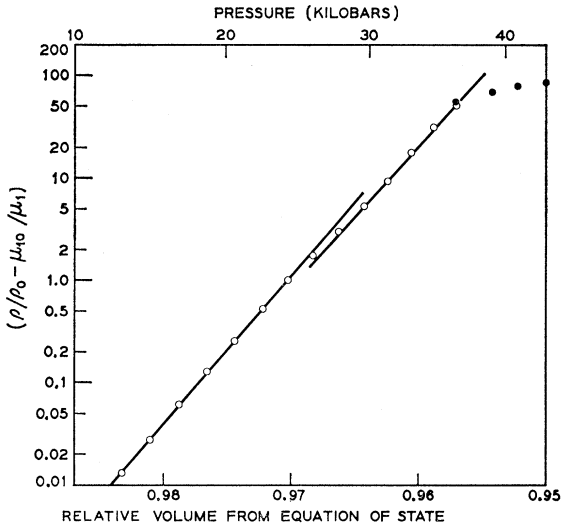

FIG. 12. The logarithm of the change in normalized resistivity due to carrier transfer and carrier freeze-out versus crystal volume for a (111) plate of sulfur-doped GaAs.

atmospheric-pressure energy separation of the band-edge points of slightly more than 0.36 eV.

We have made plots like that of Fig. 12 for a number of float-zoned samples and for pressure runs in different capsules. All of these plots were substantially identical with Fig. 12, though most of them showed more scatter of the data points at the lowest pressures. The characteristic departure of the data points from a straight line commencing at about 26 kbar, and the shape of the plot at higher pressures were reproducible and *not* of spurious origin, e.g., due to faulty pressure calibration at the higher pressures. The "dip" in the curve between 26 and 30 kbar was equally evident in the original plots against *pressure*.

We believe that the initial departure of the data just above 26 kbar is due to the onset of an appreciable contribution to the conductivity from electrons in the [100] band [the term involving $e^{-\epsilon}$ in the denominator of Eq. (9) no longer negligible]. If it were not for the "freeze-out" of carriers which takes place in the same upper pressure range, we would expect the data points to go smoothly to an asymptotic value of about 40.

It is relatively easy to show that carrier "freeze-out" must be occurring at pressures above 30 kbar. In this region the plot is essentially the same as a plot of $\ln\rho$ versus volume V. If we *assume no carrier freeze-out*, the *maximum* slope of a plot of $\log\rho$ versus V can be shown to be

$$\left(\frac{d\ln\rho}{dV}\right)_{\max}=\frac{d\epsilon}{dV}\left[\frac{b}{(b+1)^{1/2}+b}-\frac{1}{(b+1)^{1/2}+1}\right], \tag{10}$$

where b is the mobility ratio μ_1/μ_2. The straight line through the data points above 30 kbar on Fig. 12 has a slope which is 0.96 $(d\epsilon/dV)$. From Eq. (10) the

bracketed term is 0.73 for $b=40$ and 0.80 for $b=85$. Thus, "freeze-out" makes a substantial contribution to the rate of increase of resistivity above 30 kbar.

The shape of the resistivity-versus-pressure curve above 37 kbar, where it saturates, is difficult to analyze for two reasons: First, the working fluid freezes so that the additional force is seen by the sample as a uniaxial instead of a hydrostatic stress; second, the mobility of the electrons in the [000] valley may be expected to drop due to intervalley scattering when the band-edge separation gets down to 1 or 2 kT.

ACKNOWLEDGMENTS

We are indebted to J. H. McFee for his active participation in preliminary experiments, to V. C. Wade for sample preparation, and to R. G. Maines for aid in loading and operating the high-pressure apparatus.

PHYSICAL REVIEW VOLUME 155, NUMBER 3 15 MARCH 1967

Electron Mobility in Semiconducting Strontium Titanate

O. N. TUFTE AND P. W. CHAPMAN
Honeywell Corporate Research Center, Hopkins, Minnesota
(Received 18 October 1966)

The electron Hall mobility has been measured in semiconducting $SrTiO_3$ over the temperature range from 1.6 to 550°K. Electron concentrations in the range from 1×10^{17} to 2.5×10^{19} cm^{-3} were obtained by reduction or by doping with niobium. The niobium donor centers remain fully ionized down to the lowest temperatures investigated. The low-temperature mobility in niobium-doped $SrTiO_3$ is approximately 4 times larger than in reduced $SrTiO_3$ over the concentration range investigated, and mobility values up to 2.2×10^4 cm^2/V sec were measured in niobium-doped samples having electron concentrations of approximately 2×10^{17} cm^{-3}. The mobility results are compared with the behavior expected for scattering by ionized defects and polar optical lattice modes at low and high temperatures, respectively.

I. INTRODUCTION

THE electrical transport properties of semiconducting n-type $SrTiO_3$ were first investigated by Frederikse *et al.*[1] who found a band-type conduction process with an electron effective mass much greater than the free-electron mass and low-temperature mobilities greater than 1000 cm^2/V sec. Recently, other transport effects such as the piezoresistance[2] and magnetoresistance[3] effects have also been investigated but these studies have been directed toward the determination of the energy band structure rather than the carrier scattering mechanisms. The wavelength dependence of the free-carrier absorption[4] suggests that scattering by polar optical modes is dominant at room temperature but the magnitude of the measured absorption coefficient is not in agreement with theory. The electrical properties of semiconducting $KTaO_3$, which is another pseudoferroelectric having the perovskite structure, have been investigated by Wemple,[5] who finds that the temperature dependence of the electron mobility above 100°K is the same as in $SrTiO_3$. This result suggests that the scattering mechanisms are similar in these two materials. Measurements[6] of the effect of hydrostatic pressure on the electrical conductivity and dielectric constant suggest that the mobility at room temperature is limited by lattice scattering from the lowest-energy transverse optical mode in both $SrTiO_3$ and $KTaO_3$. The behavior of the electron mobility above room temperature has not been reported in either $SrTiO_3$ or $KTaO_3$.

The purpose of the present work is to make a detailed study of the electron Hall mobility in $SrTiO_3$ over a wide range of doping conditions and a wide range of temperature as a means of investigating the scattering mechanisms. The mobility has been measured from 1.5 to 550°K in niobium-doped and reduced $SrTiO_3$ samples having electron concentrations in the range from 1×10^{17} to 3×10^{19} cm^{-3}. The mobility results are compared with the behavior expected for scattering by ionized defects and polar optical lattice modes.

II. EXPERIMENTAL PROCEDURE

Single crystals of $SrTiO_3$ were obtained from the National Lead Company. The crystals were doped either by the addition of niobium during growth or by the reduction of the undoped crystals. The procedure for reducing $SrTiO_3$ has previously been described.[1,2]

[1] H. P. R. Frederikse, W. R. Thurber, and W. R. Hosler, Phys. Rev. **134**, A442 (1964).
[2] O. N. Tufte and E. L. Stelzer, Phys. Rev. **141**, 675 (1966).
[3] H. P. R. Frederikse, W. R. Hosler, and W. R. Thurber, Phys. Rev. **143**, 648 (1966).
[4] W. S. Baer, Phys. Rev. **144**, 734 (1966).
[5] S. H. Wemple, Phys. Rev. **137**, A1575 (1965).
[6] S. H. Wemple, A. Jayaraman, and M. DiDomenico, Jr., Phys. Rev. Letters **17**, 142 (1966).